Jour. Fac. Sci., Hokkaido Univ., Ser. IV,
vol. 23, no. 1, July., 1991, pp. 41-51

STUDY OF THE STRUCTURE MODEL OF TODOROKITE

by

Hiroyuki Miura

(with 5 text-figures and 3 tables)

Abstract

The X-ray diffraction study of todorokite from Japan was carried out and appropriate structural model was calculated by Rietveld method. The calculation of the theoretical diffraction pattern was done for a layer structural model and the calculated results show that the layer model can explain the observed diffraction data. Some of the properties of todorokite such as superstructure or shrinkage of c-axis on heating can be explained by the layer model which contains random H_2O between the $[MnO_6]$ layers.

Introduction

Todorokite is a manganese oxide mineral having H_2O in its structure. It was reported first from the Todoroki gold mine, Hokkaido, Japan (Yoshimura, 1934). This mineral occurs as aggregate of fine acicular crystals. It also contains H_2O, Ca, Ba and Mg. The X-ray powder diffraction data of todorokite clearly show diffraction peaks of 9.6, 4.8, 3.2, 2.45 and 1.42 Å.

Since 1934 there has been many reports of todorokite like minerals from all over the world (Frondel, 1953; Frondel et al., 1960; Ljunggren, 1960; Straczek et al., 1960; Faulring, 1961; Larson, 1962; Radtke et al., 1967; Lawrence et al., 1968; Harada, 1982; Siegel and Turner, 1983). There are many names for these types of minerals, such as "woodruffite" (Frondel, 1953), "Delatorreite" (Straczek et al., 1960), "Buserite" (Giovanoli et al., 1975). "10 Å-manganite" (Buser, 1959), which shows a similar X-ray diffraction pattern as todorokite, has been found in deep sea manganese nodules. There is confusion regarding to the definition of todorokite primarily because the crystal structure of todorokite has not been fully determined as yet.

On the basis of X-ray diffraction profiles Buser and Grutter (1956) proposed that the crystal structure of todorokite in manganese nodule has a layer structure analogous to lithiophorite. However this idea was not supported by later workers since the habit of cleavage are different in these two minerals and instead a tunnel structure model for todorokite was proposed on the basis of crystal morphology (Burns and Burns, 1977; Burns et al., 1983 and 1985) and high-resolution transmission electron microscopy (HRTEM) studies (Tuner and Buseck, 1981; Turner et

Contribution from the Department of Geology and Mineralogy, Faculty of Science, Hokkaido University, No. 2051

al., 1982).

Using Rietveld method Post and Bish (1988) recently suggested a tunnel structure model for todorokite from Cuba. However there are still problems with the tunnel structural model as follows.

Todorokite from Urizukuri changes the d-value of 001 diffraction peak from 10.08 Å to 9.56 Å on drying (Harada, 1982). Todorokite from the Todoroki mine also shows similar behavior (Miura and Hariya, 1984). The contraction is observed only in c-direction and the tunnel model can not explain their anisotropic feature of the unit cell. IR spectra of todorokite are consistent with either a layer structure of linked [MnO_6] octahedra containing vacancies, or a highly polymerized chain or tunnel structure with quadruple chains (Potter and Rossman, 1979). Cryptomelane which has tunnel structure shows fibrous needle shape (Faulring et al., 1960). Synthetic manganese oxide which has a large tunnel consisting of double and quintuple MnO_6 chains shows needle shape (Tamada and Yamamoto, 1986). Todorokite samples from Cuba show the crystals to be thin plates flattened on (001) and many of the plates are broken into thin blades elongated along [010] (Straczek et al., 1960). Todorokites from the Todoroki mine consist of narrow laths or blades elongated along [010]. They show perfect clevage parallel to 001. Therefore the crystal morphology of todorokite is different from that of manganese oxide which has tunnel structure. The crystal morphology and clevage of todorokite can be explained by a layer structural model. In this paper, the calculated X-ray powder diffraction profiles based on the layer structural model is compared with the observed diffraction data from natural samples. Also an appropriate structural model for todorokite has been suggested.

Experimental

X-ray powder diffraction study

Samples of todorokite were selected from five localities in Japan, the Todoroki mine (Hokkaido), the Ikeshiro mine (Shizuoka Prefecture), the Maruyama mine (Aomori Prefecture), Urizukuri (Yamaguchi Prefecture) and Akan-Yunotaki (Hokkaido). In the Todoroki mine, this mineral occurs as aggregates of very fine flakes of about 0.05 mm in its largest dimension (Yoshimura, 1934). It covers the wall of a druse in the oxidized zone of the gold deposit. The occurrence of the two samples from the Maruyama mine and the Ikeshiro mine are not known. Both of them are also aggregates of fine acicular crystals. In Urizukuri, Yamaguchi Prefecture, todorokite occurs in the hydrothermal alteration zone and does not show any well developed crystal habit. Under electron microscope, however, typical acicular forms have been observed (Harada, 1982). Todorokite from Akan occurs in hot spring owing to recent volcanic activity, and looks like black clay.

The X-ray powder diffraction data were collected using Cu-Kα radiation with a graphite monochromater from $2\theta=4^\circ$ to 70°. Step size was 0.05° and counting

time was 30 sec. Samples were mounted on the sample holder made up of Si single crystal plate to minimize the effect of background scattering of X-ray.

X-ray diffracction photograph of todorokite.

An X-ray diffraction photograph of acicular todorokite sample from the Todoroki mine was taken keeping the long axis vertical. As the acicular todorokite consists of crystallographically parallel grains, an X-ray diffraction photograph resembling rotation photograph was obtained. Graphite monochromated Mo-Kα radiation with 60 Kv, 200 mA was used for the experiment. The distance between specimen and flat film was 30 mm and 60 mm. The exposure time was 30 minutes. All axes of goniometer and film were fixed during exposure.

Experimental results

X-ray powder diffraction profiles of todorokite

X-ray data for todorokite from Japan are given in Table 1 and Fig. 1. It is apparent that considerable variation exists between relative intensity of comparable lines for different todorokite samples. The maximum peak intensity varies with the crystallinity. The weak and broad 7.2 Å and 4.4 Å peaks are seen in the diffraction data of todorokite from Todoroki, Ikeshiro, Maruyama and Urizukuri. Their peak intensities relative to the most intense peak are 1-2% (7.2 Å) and 2-8% (4.4 Å). The diffraction profiles of todorokite from Akan-Yunotaki do not show these diffraction peaks and indicate that its structure is different from the todoro-

Table 1 X-ray powder diffraction data for todorokites from Japan

Ikeshiro		Todoroki		Maruyama		Urizukuri		Akan	
I	d	I	d	I	d	I	d	I	d
100	9.57	100	9.67	100	9.60	100	9.56	100	9.74
1d	7.2	1d	7.2	<1d	7.2	2d	7.2	—	—
20	4.78	15	4.82	20	4.78	23	4.78	25	4.89
2d	4.4	2d	4.4	3d	4.4	8d	4.4	—	—
2	3.39	—	—	—	—	—	—	—	—
6	3.17	3	3.21	5	3.17	5	3.23	2	3.25
11	3.11	2	3.10	5	3.08	5	3.12	—	—
2d	3.0	2d	3.0	3d	3.0	—	—	—	—
<1	1.62	—	—	<1	1.65	—	—	—	—
2	1.56	—	—	—	—	—	—	—	—
<1	1.53	<1	1.54	1	1.53	<1	1.53	<1	4.46
1	1.42	1	1.42	1	1.42	1	1.42	1	1.42
1	1.39	<1	1.39	1	1.41	—	—	—	—
<1	1.37	—	—	2	1.38	1	1.37	—	—

d: diffused line

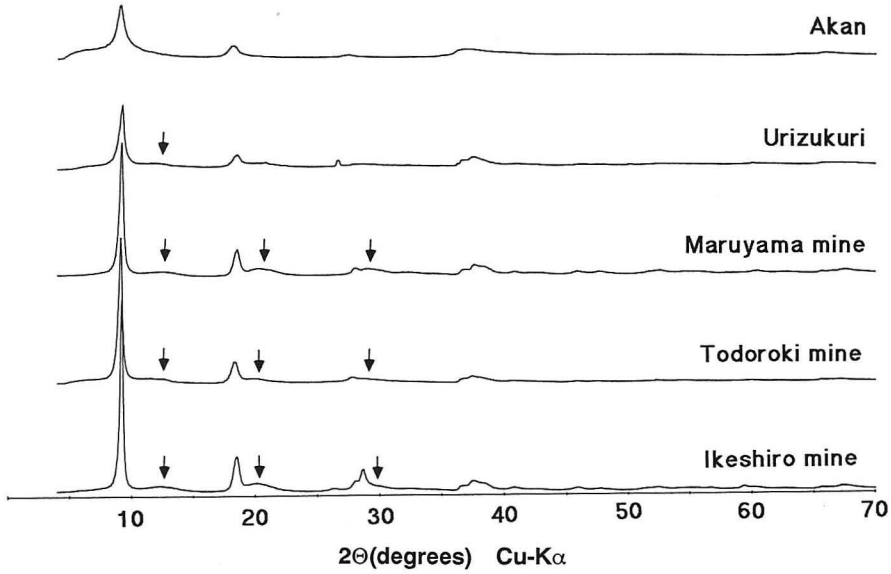

Text-fig. 1 X-ray powder diffraction profiles of todorokites from Japan. Arrows locate weak and broad diffraction peaks. Experimental conditions: Radiation: Cu-Kα, 35 Kv, 20 mA: Monochromater: graphite; Scanning method: step scanning; step size: 0.05°; Counting time: 30 sec.

kite from the Todoroki mine, the Ikeshiro mine, the Maruyama mine and Urizukuri.

The d-values of 001 diffraction peaks vary widely depending on the locality. This has been explained due to H_2O content (Harada, 1982; Miura and Hariya, 1984).

X-ray diffraction photograph of acicular todorokite.

The X-ray diffraction photographs of acicular todorokite from the Todoroki mine are shown in Figs. 2a, b. For a single crystal, the diffraction spot should not be observed on the film and the rotation of specimen is necessary to set the appropriate position for diffraction. An aggregate of fine crystals with random orientation will show concentric Debye-Scherrer rings on X-ray photograph. The X-ray diffraction photographs show weak Debye-Scherrer rings and diffraction spots. The Debye-rings are derived from fine crystals of random orientations and the spots are given by fibrous todorokite crystals. If one of the axes of many fibrous crystals are in parallel alignment but the other two axes are not preferentially oriented, the same rotational effects will occur. So, it is reasonable to assume that the specimen is aggregate of long and short crystals parallel to a certain axis. Thus it is possible to treat the photograph as a rotation photograph. The distance between the zero layer and the first layer shows that the unit cell, which is constant along the extended axis of acicular todorokite, is 2.8 Å. The specimen is elongated along the b-axis.

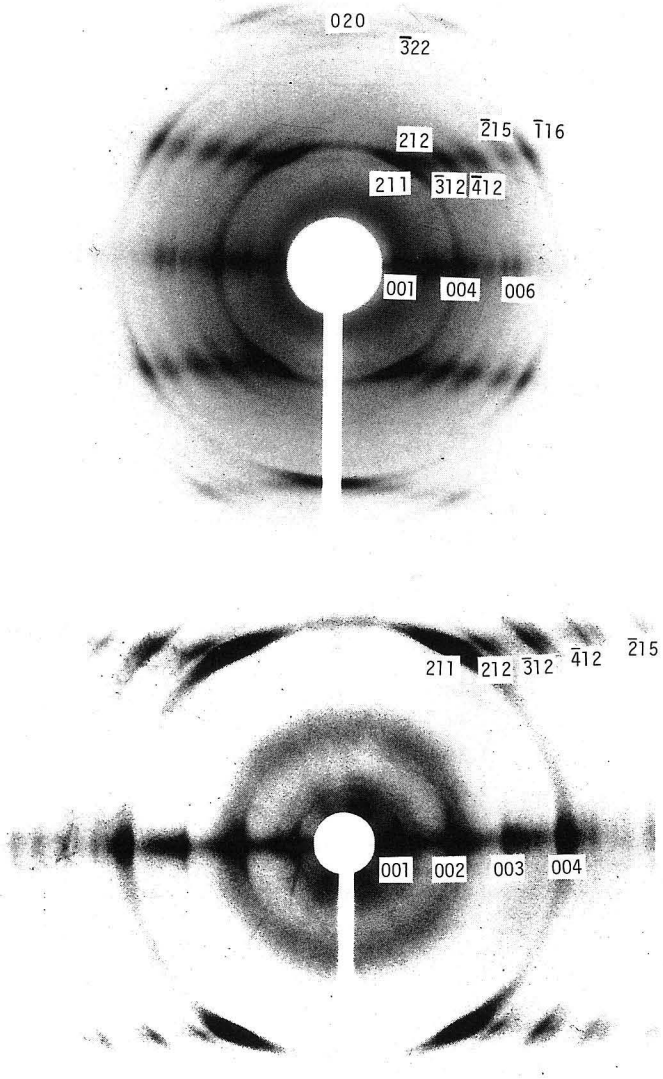

Text-fig. 2 X-ray diffraction photograph of todorokite from the Todoroki mine.
(a) distance: 30 mm
(b) distance: 60 mm

The diffraction spots on the zero layer have an index of (h 0 l) and the spots on the first layer have an index of (h 1 l). Then, all of the spots were possible to index from the observed and calculated d-value. Assuming that the symmetry is monoclinic, cell constants are refined with the powder diffraction data and Rietveld method. The cell constants are a=9.80 Å, b=2.82 Å, c=9.62 Å, β=93.7°. Table 2 shows the observed diffraction spots and the calculated indexes. The diffraction spots 001, 002, 003 and 004 have streaks and show that there is stacking faults toward a or c axis. These streaks are analogous to the weak and broad peaks

Table 2 X-ray diffraction data for acicular todorokite.

$2\theta_{obs.}$	$d_{obs.}$	$d_{calc.}$	h	k	l
4.2	9.72	9.60	0	0	1
8.4	4.84	4.80	0	0	2
12.9	3.16	3.20	0	0	3
16.8	2.43	2.41	−4	0	1
		2.40	0	0	4
19.4	2.11	2.12	4	0	2
25.0	1.64	1.60	0	0	6
32.5	1.27	1.28	−5	0	6
34.4	1.20	1.20	0	0	8
16.9	2.40	2.39	−2	1	1
		2.35	2	1	1
18.6	2.19	2.21	−2	1	2
		2.15	2	1	2
20.7	1.97	1.98	−3	1	2
		1.97	−2	1	3
23.7	1.73	1.74	−2	1	4
		1.55	−5	1	2
27.2	1.51	1.53	−5	1	2
29.5	1.39	1.39	−1	1	6
30.7	1.34	1.41	0	2	0
32.3	1.27				
34.4	1.20				

Radiation: graphite monochromated Mo-Kα.
Diffraction data are inexed based on the cell dimensions of monoclinic system (a=9.80 Å, b=2.82 Å, c=9.62 Å, β=93.7°)

observed in the powder diffraction patterns.

Calculated X-ray diffraction pattern of the layer model

Theoretical X-ray diffraction profiles based on the layer structure model were calculated to check if this crystal model is consistent with the observed X-ray diffraction data. The layer structure consists of layers of edge-shared [MnO_6] octahedra. The distance between two layers of [MnO_6] octahedra is about 9.6 Å along the c-axis. Todorokite contains a significant H_2O in its structure. Stouff and Boulegue (1988) proposed the structural model of the synthetic 10-Å phyllomanganate which contains H_2O layers in between [MnO_6] octahedron layers. Todorokite contains about 10% H_2O and its location is assumed to be similar to 10 Å phyllomanganate. The chemical analyses of todorokite (Yoshimura, 1936) give the chemical formula as $Ca_{0.8}Mn_4O_8 \cdot 2H_2O$. The program RIETAN (Izumi, 1985) was used to obtain the X-ray diffraction profile. Back ground parameters, preferred orientation parameters, cell constants, fractional coordinates X of Ca, X

and Z of Mn(2), thermal parameters of Ca, Mn, O and H_2O were refined using RIETAN. H_2O atoms are represented by oxygen in calculation. There are 4 symmetry-independent positions for H_2O in a unit cell of Stouff's model (1 : 0.083, 0.500, 0.373 ; 2 : 0.167, 0.0, 0.627 ; 3 ; 0.333, 0.5, 0.373 ; 4 : 0.417, 0.0, 0.627) (Stouff and Boulegue, 1988). For the positions of H_2O, two structural models are compared. The model which has H_2O in position 1 and 2 (occupancy rate is 0.5) shows better agreement than the model which have H_2O in positions 1, 2, 3 and 4 (occupancy rate is 0.25). Therefore H_2O molecules are assumed to be in the positions 1 and 2. The final R. F. is reduced to 4.9%. The calculated crystallographic data of the layer model are listed in Table 3. Rietveld refinement shows that the crystal system is monoclinic and the cell constants are a=9.80(3) Å, b=2.822(6) Å, c=9.62 (1) Å and β=93.7(2)°. Fig. 3 shows the calculated X-ray diffraction profile and observed data of todorokite from Todoroki mine. The observed data shows the weak and broad peaks of 7.2, 4.4 and 2.9 Å which is caused by the disorder toward a- or c-axis. As the structural model does not take into account the disorder along a- or c-axis, the calculated and observed profiles are not well matched in this region. Generally however, the calculated diffraction profile of the layer model shows good agreement to the observed data of natural todorokite. So it is reasonable to conclude that todorokites from the Todoroki mine, and other localities in Japan have a layer structure.

Table 3 Crystallographic data for layer structure model.

Crystal system : monoclinic
Space Group : P2/m

Atomic coordinate

	X	Y	Z	B	Occ
Ca	0.265	0.500	0.500	4.8	0.4
Mn1	0.000	0.000	0.000	1.6	1.0
Mn2	0.216	0.500	0.017	0.7	1.0
Mn3	0.500	0.000	0.500	0.7	1.0
O1	0.096	0.500	0.890	36.4	1.0
O2	0.154	0.000	0.110	36.4	1.0
O3	0.346	0.000	0.890	36.4	1.0
O4	0.404	0.500	0.110	36.4	1.0
H_2O1	0.083	0.500	0.373	−17.3	0.5
H_2O2	0.167	0.000	0.627	−17.3	0.5

Cell constants

a = 9.80 (3) Å
b = 2.822(6) Å
c = 9.62 (1) Å
β = 93.7 (2) °

Formula $Ca_{0.8}Mn_4O_8 \cdot 2H_2O$
Z=4
D_{calc}= 2.48 g/cm^3

Standard deviations on the last digits are given in parentheses.

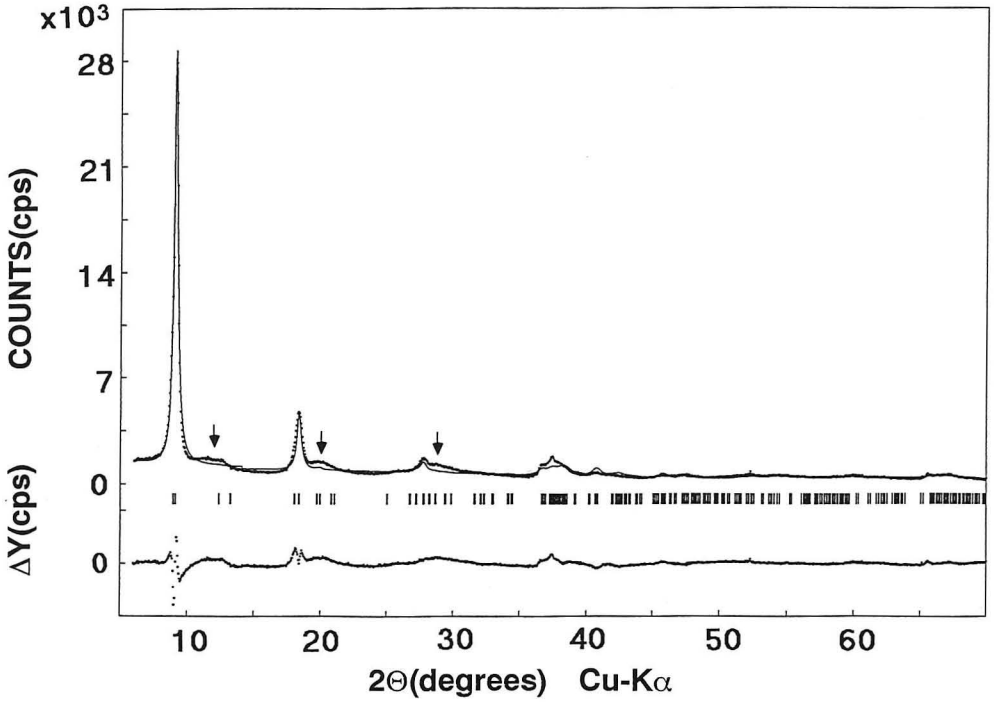

Text-fig. 3 Observed and calculated diffraction profiles of todorokite from Todoroki mine. The dots are observed data and solid lines are calculated profiles. The vertical bar-marks indicate the positions of the calculated diffraction peaks. The difference between the observed and the calculated data (ΔY) is plotted below the vertical barmarks. Arrows locate the observed weak and broad diffraction peaks derived from the disorder toward a or c direction.

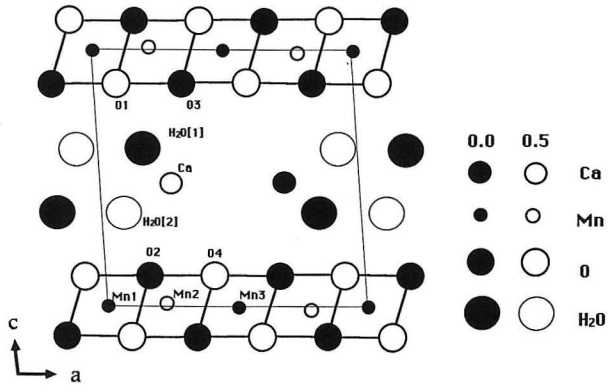

Text-fig. 4 Projection down b of todorokite crystal structure. The light line show the unit cell. In this model, the occupancy of $H_2O[1]$, $H_2O[2]$ and Ca are 0.5, 0.5 and 0.4, respectively.

Discussion

The structural model of todorokite

The 3×3 structure model can explain the observed pattern (Post and Bish, 1988). Further the layer model which contains H_2O between [MnO_6] layers can also explain the observed pattern.

Heat treatment of todorokite shows that the d-spacing of the (001) diffraction peaks of todorokite from Urizukuri decrease when dried (Harada, 1982). Todorokite from the Todoroki mine also show decrease in d-spacing of (001) diffraction peaks when heated (Miura and Hariya, 1984). If todorokite has a 3×3 tunnel structure and the arrangement of [MnO_6] octahedron is similar to both a-axis and c-axis directions then both axes should contract simultaneously. However in the experiment, only c-axis contracts after heating, Indicating that the arrangement of atom in todorokite is different in the a- and c-axis directions. Hollandite and cryptomelane have tunnel structures consisting of double chains of [MnO_6] octahedra. H_2O molecules occupy the tunnel sites and are released during heating without decrease of cell dimension (Miura, 1986). Therefor the observed data agree better with the layer model than with the tunnel model.

Super structure of todorokite

The broadness of the X-ray diffraction peaks of 7.2 Å and 4.4 Å can be explained by disorder in the position of H_2O and metal element. The arrangement of the inter layer element will make superstructure towards a-axis. In a structure of well crystallized todorokite, H_2O and metal atom will exist at regular intervals. Fig. 5 show a schematic diagram of the layer structure model having different distance between H_2O molecules. A rectangular represents [MnO_6] octahedron. Each octahedron shifts by 1/2 b alternately as shown by white and black. The length of one octahedron in the direction of a-axis is 2.47 Å. If H_2O exist at exery 5 octahedron, the group of H_2O shift 1/2 b alternately depending on the position of octahedron in layer (Fig. 5b). So 12.3(=2.47×5) Å should not be the length of a- axis. If the group of H_2O exist at exery 7 or 9 octahedron, 17.3(=2.47×7) Å or 22.2(=2.47×9) Å will not be an a-axis in a similar manner. In this model, the length of a -axis is multiples of 4.94(=2.47×2) Å. The polymorph of todorokite reported by Chukhrov et al. (1978) can be explained by this model.

Crystal habit of todorokite also can be explained by this model. As todorokite has a layer structure parallel to (001), flakes of todorokite exhibit a platy habit (Straczek et al., 1960). There is a disorder towards a-axis based on the position of H_2O, todorokite has a cleavage parallel to the (100) plane. The nature of these two cleavage are different. So the shape of a todorokite crystal is narrow lath or blade elongated along b-axis.

Acknowledgments

The author wishes to express his sincere gratitude to Professor Yu Hariya of

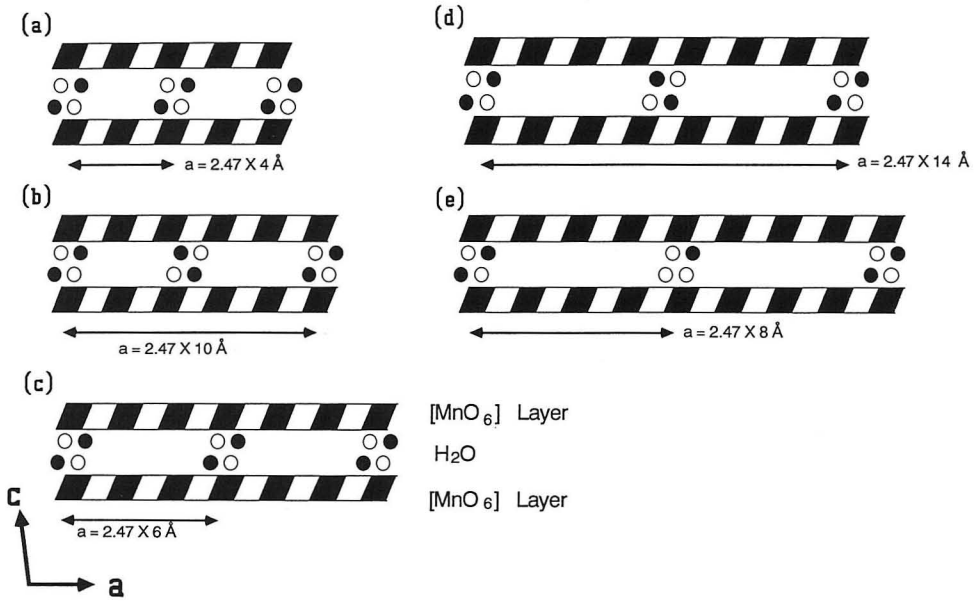

Text-fig. 5 Schematic diagrams of layer structure models. The line below each model in dicates the length of a-axis.
(a) a=9.87 Å (b) a=24.7 Å (c) a=14.8 Å
(d) a=34.5 Å (e) a=19.7 Å
A small diamond represents one [MnO_6] octahedron. A circle represents one H_2O molecule and they shift 1/2 b alternately as shown by white and black depending on the position of [MnO_6].

Hokkaido University for discussion on the subject. He is also indebted to Dr. K. Sakurai who kindly provided the samples from the Ikeshiro mine and the Maruyama mine. Thanks are also due to Professor G. Shibuya of Yamaguchi University for his kind help on the study of todorokite from Urizukuri.

References

Burns, R. G. and Burns, V. M., 1977. Mineralogy of manganese nodules. In: G. P. Glasby (Editor), *Marine Manganese Deposits*. Elsevier, Now York, 185-248.

Burns, R. G., Burns, V. M. and Stockman, H. W., 1983. A review of the todorokite-buserite problem: implications to the mineralogy of marine manganese nodules, *Am. Mineral.*, 68: 972-980.

Burns, R. G., Burns, V. M. and Stockman, H. W., 1985. The todorokite-buserite problem: further considerations, *Am. Mineral.*, 70: 205-208.

Buser, W., 1959. The nature of the iron and manganese compounds in manganese nodules. In: M. Sears (editor), *Internat. Oceanogr. Congr.*, AAA: 962-963.

Buser, W. and Grütter, A., 1956. Uber die nature der manganknollen, *Schweiz. Min. Petr. Mitt.*, 36: 49-62.

Chukhrov, F. V., Gorshkov, A. I., Sivtsov, A. V. and Beresovskaya, V. V., 1978. Structural varieties of todorokite, *Izvestia Akademia Nauk, S. S. S. R., Series Geology*, 12: 86-95.

Faulring, G. M., 1961. A study of cuban todorokite, *Advance in X-ray analysis*, 5: 117-126.

Faulring, G. M., Zwicker, W. K. and Forgeng, W. D., 1960. Thermal transformations and properties of cryptomelane, *Am. Mineral.*, 45: 946-959.

Frondel, C., 1953. New manganese oxides: hydrohausmannite and woodruffite, *Am. miner.*, 38: 761-769.

Frondel, C., Marvin, V. B. and Ito, J., 1960. New occurrence of todorokite, *Am. Miner.*, 45: 1167-1173.

Giovanoli, R., 1985. A review of the todorokite-buserite problem: implications to the mineralogy of marine manganese nodules: discussion, *Am. Miner.*, 70: 202-204.

Giovanoli, R., Bruki, P., Giuffredi. M. and Stumm, W., 1975. Layer structured manganese oxide hydroxides. IV. The buserite Group: structure stabilization by transition elements. *Chimia*, 29: 517-520.

Harada, S., 1982. Todorokite from Urizukuri, Kamikawa-mura, Abu-gunn: *Journ. of Geol. Soc. of Yamaguchi Pref.* 10: 1-6. (in Japanese)

Izumi, F., 1985. Rietveld analysis of X-ray and neutron diffraction patterns. *Journ. Miner, Soc. Japan*, 17: 37-50. (in Japanese with English abstract)

Larson, L. T., 1962. Zinc-bearing todorokite from Philipsburg, Montana. *Am. Miner.*, 47: 59-66.

Lawrence, L. J., Bayliss, P. and Tonkin, P., 1968. An occurrence of todorokite in the deuteric stage of a basalt. *Miner. Mag.*, 36: 757-760.

Ljunggren, P., 1960. Todorokite and pyrolusite from Vermlands, Sweden. *Am. Miner.*, 45: 235-238.

Miura, H, 1986. The crystal structure of hollandite. *Mineral. J.*, 13: 119-129.

Miura, H. and Hariya, Y., 1984. Todorokite with long spacing and structure of manganese dioxide minerals. *Journ. Miner. Soc. Japan*, 16: 30-308. (in Japanese with English abstract)

Post, J. E. and Bish, D. L., 1988. Rietveld refinement of the todorokite structure. *Am. Miner.*, 73: 861-869.

Potter, R. M. and Rossman, G. R., 1979. The tetravalent manganese oxides: identification, hydration and structural relationships by infrared spectroscopy. *Am. Miner.*, 64: 1199-1218.

Radtke, A. S., Taylor, C. M. and Hewett, D. F., 1967. Aurorite, Argentian todorokite and hydrous silver-bearing lead manganese oxide. *Econ. Geol.*, 62: 186-206.

Siegel, M. D. and Turner, S., 1983. Crystalline todorokite associated with biogenic debris in manganese nodules, *Science*, 219: 172-174.

Stouff, P. and Boulegue, J., 1988. Synthetic 10-Å and 7-Å phyllomanganates: Their structures as determined by EXAFS. *Am. Miner.*, 73: 1162-1169.

Straczek, J. A., Horen, A., Ross, M. and Warshaw, C. M., 1960. Studies of the manganese oxides. IV. todorokite. *Am. Miner.*, 45: 1174-1184.

Tamada, O. and Yamamoto, N., 1986. The crystal structure of a new manganese dioxide ($Rb_{0.27}MnO_2$) with a giant tunnel. *Mineral. J.*. 13: 130-140.

Turner, S. and Buseck, P. R., 1981. Todorokite: A new family of naturally occurring manganese oxides. *Science*, 212: 1024-1027.

Tuener, S., Siegel, M. D. and Buseck, P. R., 1982. Structural feature of todorokite intergrowth in manganese nodules. *Nature*, 296: 841-842.

Yoshimura, T., 1934. "Todorokite", a new manganese mineral from the Todoroki mine, Hokkaido, Japan. *Journ. Faculty Sci. Hokkaido Imp. Univ., Ser IV*, 2: 289-297.

(Manuscript received on October 26, 1990; and accepted on April 8, 1991)